Photocatalysis

DOI: 10.1002/anie.200904876

Probing Photocatalytic Active Sites on a Single Titanosilicate Zeolite with a Redox-Responsive Fluorescent Dye**

Takashi Tachikawa, Soichiro Yamashita, and Tetsuro Majima**

Microporous titanosilicate ETS-10 is a promising material for applications such as adsorption, ion exchange, and (photo)catalysis because of 1) the inherent quantum nature of one-dimensional titania (-Ti-O-Ti-) wires in the framework and 2) its high reaction selectivity owing to its pore structure (dimensions of 0.8 nm × 0.5 nm).[1–3] In a defect-free crystal, charge carriers, that is, electrons and holes, are generated by the irradiation with photons with an energy corresponding to the band gap of approximately 4 eV. These carriers migrate in the crystal through the wires. However, the wires are broken at random points in the crystal because of inherent defects; these defects form active centers for molecular adsorption and redox reactions.[3–6] To date, the influences of structural defects in ETS-10 on the adsorption and reaction dynamics of organic compounds have not been well characterized, possibly because of the heterogeneous distribution of active sites in the material.

Herein, we describe the in situ fluorescence imaging of photocatalytic oxidation on single ETS-10 crystals using a redox-responsive fluorescent dye, 3′-(*p*-aminophenyl)fluorescein (APF, Figure 1 A). APF, which was originally developed as a fluorescent probe for selective detection of the hydroxyl radical (·OH) or hypohalites,[7] was employed to identify the surface active sites distributed over the ETS-10. It was revealed that surface treatment of ETS-10 with diluted aqueous hydrofluoric acid (HF) significantly increased not only the adsorption and reaction efficiencies but also the heterogeneity of photocatalytic activity among the crystals. Furthermore, we confirmed that crystal defects serve as active sites during the photocatalytic reaction in aqueous solution.

We first tested the photocatalytic activity of samples at the bulk level. Synthetic procedures and structural characterization of ETS-10 materials are provided in the Supporting Information. As shown in Figure S3 A in the Supporting Information, the fluorescence intensity of fluorescein increased gradually upon UV irradiation of phosphate buffer solutions (pH 7.4) containing APF (500 nM) and ETS-10 powder (0.5 mg mL^{-1}). In the absence of ETS-10, the fluorescence intensity did not increase at all, thus suggesting that fluorescein molecules might be generated by the reaction of photoexcited ETS-10 and APF molecules. Meanwhile, as expected, a significant increase in the fluorescence intensity was observed for HF-treated ETS-10 because of the exposure of surface active sites such as titanols and larger micropores (supermicropores) by partial dissolution of siliceous walls surrounding the titania wires.[3] It was estimated that approximately 70 % of fluorescein molecules were generated by a bimolecular reaction with ·OH using DMSO as a scavenger (Figure S3 in the Supporting Information).

Before performing the imaging study for single ETS-10 crystals, we examined the redox responsiveness of APF using an in situ spectroelectrochemical technique combined with total internal reflection fluorescence microscopy (TIRFM, Figure 1 B).[8] According to the literature,[7a] the fluorescence of APF in aqueous solution is almost completely quenched by

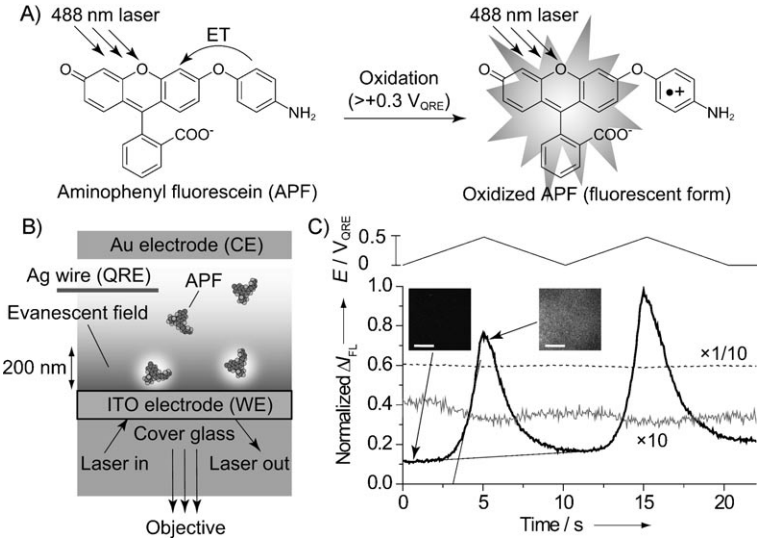

Figure 1. A) Reaction scheme for the one-electron oxidation of the *p*-aminophenyl moiety, which induces fluorescence in APF. ET = electron transfer. B) Cell configuration for in situ spectroelectrochemical measurements under TIRFM. CE = counter electrode, QRE = quasi-reference electrode, WE = working electrode. C) Applied potential dependence of normalized fluorescence intensity (I_{FL}) obtained for the phosphate buffer solutions in the absence (gray line) and presence of APF (5 μM; solid line) or fluorescein (500 nM; dashed line). The images in (C) were acquired at a bin time of 50 ms. Scale bars are 5 μm.

[*] Dr. T. Tachikawa, S. Yamashita, Prof. Dr. T. Majima
The Institute of Scientific and Industrial Research (SANKEN)
Osaka University, Mihogaoka 8-1, Ibaraki, Osaka 567-0047 (Japan)
Fax: (+81) 6-6879-8499
E-mail: tachi45@sanken.osaka-u.ac.jp
majima@sanken.osaka-u.ac.jp

[**] We are grateful to Mr. Kazuya Naito for his experimental assistance. This work has been partly supported by a Grant-in-Aid for Scientific Research (Project 17105005, 21750145, and others) from the Ministry of Education, Culture, Sports, Science and Technology (MEXT) of Japanese Government.

Supporting information for this article is available on the WWW under http://dx.doi.org/10.1002/anie.200904876.

© 2009 Wiley-VCH Verlag GmbH & Co. KGaA, Weinheim

These are not the final page numbers!

an electron-rich *p*-aminophenyl group ($\phi_{FL} = 0.008$). As demonstrated in Figure 1C, however, the fluorescence intensity of the APF phosphate buffer solution was greatly enhanced by applying a positive potential ($0 \leftrightarrow +0.5\,V_{QRE}$, where a silver wire was used as a quasi-reference electrode (QRE)). The onset of the increase in the fluorescence intensity at around $+0.35\,V_{QRE}$ can be easily correlated to the oxidation potential (E_{ox}) of aniline ($+0.36\,V_{QRE}$ ($+0.63\,V_{NHE}$; NHE = normal hydrogen electrode)),[9] which is much lower than that of fluorescein ($+1.1\,V_{NHE}$, Figure S4 in the Supporting Information),[10] thereby supporting the reaction scheme depicted in Figure 1A.

On the basis of these experimental results, we evaluated the photocatalytic activity of individual ETS-10 crystals by imaging the fluorescence generated by oxidized APF molecules during UV irradiation. Figure 2A shows typical transmission and fluorescence images of a single ETS-10 crystal in 500 nM APF phosphate buffer (pH 7.4). As predicted by ensemble experiments, the fluorescence intensity underwent a substantial increase immediately after UV irradiation, with a subsequent slight decrease (inset of Figure 2B).

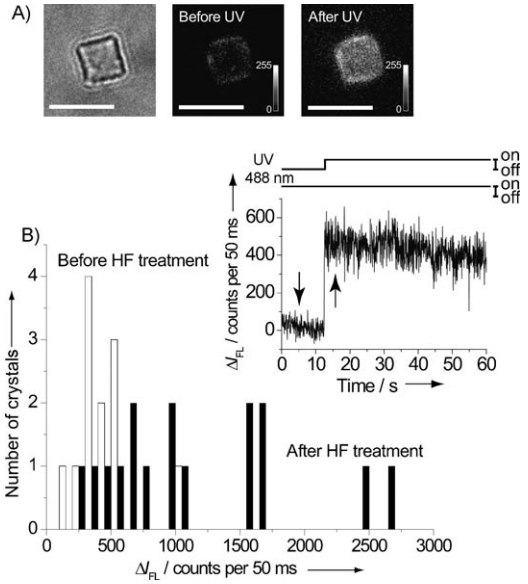

Figure 2. A) Transmission image (left) and fluorescence images of the ETS-10 crystal before (middle) and after UV irradiation (right). The arrows in the inset of (B) denote the times when fluorescence images were acquired. Scale bars are 5 μm. B) Histograms of the increase in fluorescence intensity. The white and black bars indicate histograms obtained for untreated and HF-treated ETS-10 crystals, respectively. Inset shows the time trace of differential fluorescence intensity (ΔI_{FL}), which was obtained by subtracting the background signal from the original intensity averaged over the entire ETS-10 crystal. The intensity before UV irradiation was set to zero.

We investigated the dependence of APF concentration on the fluorescence intensity for a single ETS-10 crystal (Figure S5 in the Supporting Information). Our results showed a clear linear relationship between APF concentration and fluorescence intensity; furthermore, it was estimated that the contribution of scattered light from UV irradiation was approximately 100 counts. From an overall perspective, it appears that the edge of the crystal was relatively more sensitive to UV light than the center, where the imaging focal plane was located. Furthermore, when the crystal was illuminated by evanescent light (penetration depth ca. 200 nm), the entire irradiated area on the bottom surface of the crystal exhibited similar activity as with UV light. Considering the fact that the fluorescein molecule is much larger than the ETS-10 pores, we can conclude that APF molecules are preferentially adsorbed on the exterior surface of ETS-10.[11,12]

To ascertain the origin of reactive species, we performed several control experiments. In the presence of DMSO (5 mM) as an ·OH quencher,[7b] the increase in fluorescence intensity upon UV irradiation was slightly suppressed, thereby indicating that fluorescein molecules generated from the bimolecular reaction between APF and ·OH are not readily detected owing to the rapid diffusion of free fluorescein molecules into the bulk solution.[7b] In contrast, in the presence of aniline (5 mM) as a co-adsorbate, the increase in fluorescence intensity upon UV irradiation was completely suppressed (Figure S6A in the Supporting Information). We also found that there was no significant difference in fluorescence intensity before and after the addition of benzoic acid (5 mM), thus implying that the *p*-aminophenyl group of APF plays an important role in the adsorption on the surface of ETS-10 (Figure S6B in the Supporting Information).[13]

To compare the photocatalytic activity of ETS-10 before and after HF treatment, we examined the histogram of the fluorescence intensity change for individual ETS-10 crystals. As illustrated in Figure 2B, the results for untreated ETS-10 showed a relatively narrow distribution at around 300–500 counts, while HF-treated ETS-10 had a significantly broader distribution (250–2750 counts). We confirmed this increase in fluorescence intensity for a selected ETS-10 crystal in APF buffer solution after HF treatment (Figure S7 in the Supporting Information). Single-crystal Raman spectroscopy measurements also support the hypothesis that the partial dissociation of titania wires in ETS-10 by HF treatment produces the surface active sites (Figure S8 in the Supporting Information).[3]

Experiments on a single crystal provide useful information for elucidating the inherent heterogeneity of reaction processes occurring at the solid–liquid interface. Figure 3 shows an example of the influence of crystal defects on the photocatalytic oxidation of APF molecules. Figure 3A shows transmission (left) and fluorescence (right) images acquired for one single HF-treated ETS-10 crystal. The spatial configuration of the crystal is also illustrated in Figure 3B. To confirm the existence of defects, we carefully analyzed the transmission images acquired at different focal planes.

Figure 3C shows time traces of the fluorescence intensity acquired at a crack-like defect (position 1) and at a point near the edge (position 2). The increase in fluorescence intensity observed at the defect upon UV irradiation is considerably higher than the increase observed at position 2 and other areas. This finding obviously reflects the fact that crystal defects in ETS-10, where titanols and supermicropores are probably present,[5] yield highly active sites for adsorption and oxidation of organic compounds.

 © 2009 Wiley-VCH Verlag GmbH & Co. KGaA, Weinheim

These are not the final page numbers!

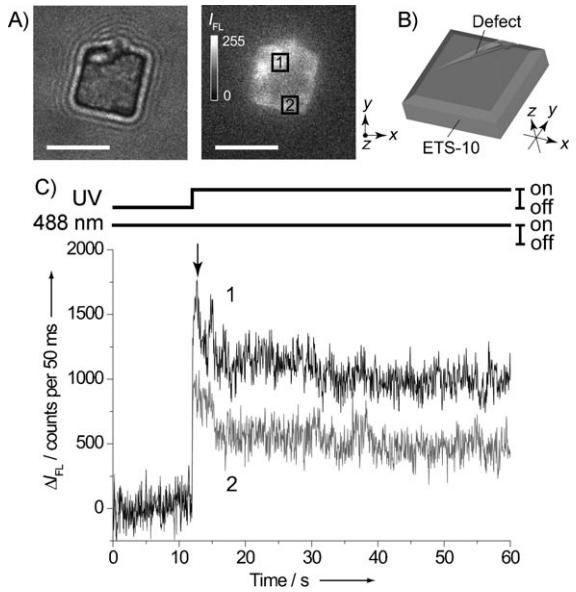

Figure 3. A) Transmission image (left) and fluorescence image under UV irradiation (right), where the imaging focal plane was located at the center of the crystal. The arrow in (C) denotes the time when the fluorescence image was acquired. Scale bars correspond to 5 μm. B) Spatial configuration of the crystal (see the axes). C) Time traces of the fluorescence intensity acquired at the defect (position 1, black line) and near the edge of the ETS-10 crystal (position 2, gray line). Additional data are provided in the Supporting Information (Figure S9).

We further examined the influence of accumulation of intermediates or products on the turnover number for photocatalysis on a single crystal. Figure 4 shows time traces

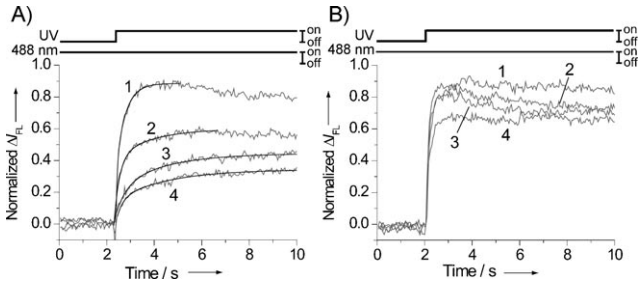

Figure 4. Time traces of fluorescence intensity repeatedly acquired for A) an untreated and B) an HF-treated ETS-10 crystal (gray lines). Numbers refer to the repetition number. Black lines indicate biexponential curves fitted to the time traces.

of the fluorescence intensity acquired repeatedly for the same ETS-10 crystal. For the untreated ETS-10 crystal, the increase in fluorescence intensity was clearly suppressed by repeating a given sequence, that is, flow of substrate solution (40 μL × 3), data acquisition (488 nm laser irradiation for 10 s and UV irradiation for 8 s), and waiting for 1 min (Figure 4 A). It is noteworthy that the rise times of fluorescence intensity increased because of frequent repetition.

The time traces were tentatively fitted using a nonlinear least-squares method with a biexponential function given by $I_{FL}(t) = a_1 \exp(-t/\tau_1) + a_2 \exp(-t/\tau_2)$, where I_{FL} is the fluorescence intensity, a is the preexponential factor, and τ is the rise time. As summarized in Table 1, weight-average rise times $\langle\tau\rangle$[14] for untreated ETS-10 increased considerably with an increase in the number of repetitions. On the other hand, as shown in Figure 4 B, similar tendencies were not observed for most HF-treated ETS-10 crystals. The $\langle\tau\rangle$ values for HF-treated ETS-10 exhibited no significant change under the same reaction conditions ($\langle\tau\rangle = 100$–200 ms).

Table 1: Fitting parameters for time traces of the fluorescence intensity observed for a single untreated ETS-10 crystal.

Repetition	τ_1 [s] (a_1 [%])	τ_2 [s] (a_2 [%])	$\langle\tau\rangle$ [s][a] ($\langle\tau\rangle^{-1}$ [s^{-1}])
1	0.392 (45)	0.0459 (55)	0.35 (2.9)
2	0.225 (64)	1.54 (36)	1.3 (0.77)
3	0.434 (45)	2.05 (55)	1.8 (0.56)
4	0.244 (45)	2.13 (55)	2.0 (0.50)

[a] Error within ±10%. The response time of the instrument is less than 100 ms.

The photocatalytic reaction mechanism proceeds according to the reactions in Equations (1)–(4):

$$\text{ETS-10} + h\nu \rightarrow e^- + h^+ \quad (1)$$

$$e^- + Ti^{4+} \rightarrow Ti^{3+} \quad (2)$$

$$h^+ + APF_{ads} \rightarrow \text{oxidized } APF_{ads} \text{ (fluorescent form)} \quad (3)$$

$$\text{oxidized } APF_{ads} + h^+ \text{ or ROS} \rightarrow \text{products} \quad (4)$$

Upon irradiation with UV light, the generated electrons (e^-) and holes (h^+) are transferred to electron trapping sites such as Ti^{4+} and APF molecules adsorbed on the surface of the crystal [Eqs. (1–3)]. Both free and surface-trapped h^+ might be included in the oxidation process.[15] Upon oxidation of the *p*-aminophenyl group, APF molecules attain the fluorescent form in a manner similar to the fluorescein molecule. The generated emissive APF-based molecules are further oxidized by h^+ or reactive oxygen species (ROS) to give adsorbed products [Eq. (4)]. This situation should inhibit the adsorption of free APF molecules on the surface, thereby resulting in a decrease in photocatalytic activity. For highly active ETS-10, that is, HF-treated samples, fresh APF molecules are continually supplied to the active sites from the surroundings, because most products are decomposed and desorbed from the surface into the bulk solution.

In conclusion, we have demonstrated in situ fluorescence imaging of photocatalytic active sites heterogeneously distributed on individual ETS-10 crystals using redox-responsive APF molecules. Our strategy can be employed in single-molecule turnover experiments to investigate heterogeneous photocatalysis.[16] Such studies are currently in progress.

Experimental Section

ETS-10 was hydrothermally synthesized according to the procedure reported by Yoon et al.[2] A suspension of anatase TiO_2 nanoparticles was added to a mixture of sodium silicate (8.5 g), sodium hydrate (2.6 g), and Milli-Q water (75 mL) with vigorous stirring. A mixture

© 2009 Wiley-VCH Verlag GmbH & Co. KGaA, Weinheim

of potassium fluoride (1.7 g) and Milli-Q water (15 mL) was added to this mixture, and the resulting suspension was maintained at room temperature for 18 h. A portion of the suspension was heated in a Teflon-lined autoclave at 200 °C for 72 h. The resulting material was separated by centrifugation, repeatedly washed with Milli-Q water until pH 7, and then dried overnight at 90 °C.

Synthesized ETS-10 powder was rapidly mixed with 8 wt % HF, and the mixture was vigorously stirred for 3 s and added into excess Milli-Q water.[3a] (It should be noted that HF is extremely corrosive and behaves as a contact poison; hence, it should be handled with extreme care.) The resulting material was separated by centrifugation, repeatedly washed with Milli-Q water until pH 7, and then dried overnight at 90 °C. Experimental details and spectroscopic data (SEM, powder XRD, and UV/Vis diffuse reflectance spectra) of the ETS-10 materials are provided in the Supporting Information.

For single-molecule, single-crystal fluorescence measurements, an aqueous suspension of ETS-10 crystals was cast on a clean cover glass by spin coating. The coated cover glass was annealed and washed with Milli-Q water. The cover glass was placed on a flow cell built in-house.

The experimental setup for single-particle experiments is based on an Olympus IX71 inverted fluorescence microscope.[7b] Continuous-wave laser light (488 nm) passing through an objective lens (Olympus, UPlanSApo, 1.40 NA, 100×) after reflection at dichroic mirrors was used to excite fluorescent probes. For UV excitation of the sample, light emitted from a 100 W mercury lamp that passed through a 340 nm bandpass filter and a 6% ND filter was made incident on an object lens. For imaging, fluorescence was collected using an objective, passed through emission filters to remove undesirable scattered light, and imaged by an EM-CCD camera (Roper Scientific, Cascade II:512) at a frame rate of 20 frames s^{-1}.

For single-crystal Raman spectroscopy, 532 nm CW laser light passing through an objective lens after reflection at a dichroic mirror was used to excite crystals. The scattered light as well as a background emission was collected using the same objective, passed through an emission filter to remove scattered excitation light and a slit, and entered the imaging spectrograph (Acton Research, SP-2356) that was equipped with an EM-CCD camera (Princeton Instruments, PhotonMAX:512B).

In situ spectroelectrochemical measurements were carried out at room temperature using an electrochemical analyzer (ALS, model 660 A) with a standard three-electrode configuration (Figure S4 in the Supporting Information).[8b] All the experimental data were obtained at room temperature.

Received: September 1, 2009
Published online: ■■ ■■, 2009

Keywords: fluorescent probes · heterogeneous catalysis · photochemistry · single-particle studies · zeolite analogues

[1] M. W. Anderson, O. Terasaki, T. Ohsuna, A. Philippou, S. P. MacKay, A. Ferreira, J. Rocha, S. Lidin, *Nature* **1994**, *367*, 347 – 351.

[2] N. C. Jeong, M. H. Lee, K. B. Yoon, *Angew. Chem.* **2007**, *119*, 5972 – 5976; *Angew. Chem. Int. Ed.* **2007**, *46*, 5868 – 5872.

[3] a) F. X. Llabrés i Xamena, P. Calza, C. Lamberti, C. Prestipino, A. Damin, S. Bordiga, E. Pelizzetti, A. Zecchina, *J. Am. Chem. Soc.* **2003**, *125*, 2264 – 2271; b) S. Usseglio, P. Calza, A. Damin, C. Minero, S. Bordiga, C. Lamberti, E. Pelizzetti, A. Zecchina, *Chem. Mater.* **2006**, *18*, 3412 – 3424.

[4] P. D. Southon, R. F. Howe, *Chem. Mater.* **2002**, *14*, 4209 – 4218.

[5] C. C. Pavel, S.-H. Park, A. Dreier, B. Tesche, W. Schmidt, *Chem. Mater.* **2006**, *18*, 3813 – 3820.

[6] L. Lv, J. K. Zhou, F. Su, X. S. Zhao, *J. Phys. Chem. C* **2007**, *111*, 773 – 778.

[7] a) K. Setsukinai, Y. Urano, K. Kakinuma, H. J. Majima, T. Nagano, *J. Biol. Chem.* **2003**, *278*, 3170 – 3175; b) K. Naito, T. Tachikawa, M. Fujitsuka, T. Majima, *J. Am. Chem. Soc.* **2009**, *131*, 934 – 936; c) V. Martínez Martínez, G. De Cremer, M. B. J. Roeffaers, M. Sliwa, M. Baruah, D. E. De Vos, J. Hofkens, B. F. Sels, *J. Am. Chem. Soc.* **2008**, *130*, 13192 – 13193.

[8] a) R. E. Palacios, F.-R. F. Fan, A. J. Bard, P. F. Barbara, *J. Am. Chem. Soc.* **2006**, *128*, 9028 – 9029; b) T. Tachikawa, T. Majima, *J. Am. Chem. Soc.* **2009**, *131*, 8485 – 8495.

[9] P. Winget, E. J. Weber, C. J. Cramer, D. G. Truhlar, *Phys. Chem. Chem. Phys.* **2000**, *2*, 1231 – 1239.

[10] J. Suomi, T. Ylinen, M. Håkansson, M. Helin, Q. Jiang, T. Ala-Kleme, S. Kulmala, *J. Electroanal. Chem.* **2006**, *586*, 49 – 55.

[11] a) As a separate experiment, we studied the adsorption behavior of fluorescein molecules on the surface of ETS-10 powders in solutions, and we estimated the number of adsorbed fluorescein molecules to be less than 5% and approximately 10% of the total molecules (500 nM) in the untreated and HF-treated ETS-10 powders, respectively. Experimental procedures were described elsewhere; b) T. Tachikawa, Y. Asanoi, K. Kawai, S. Tojo, A. Sugimoto, M. Fujitsuka, T. Majima, *Chem. Eur. J.* **2008**, *14*, 1492 – 1498.

[12] a) In general, when fluorescein molecules are adsorbed on the TiO_2 surface, the fluorescence signals from fluorescein cannot be observed because of the excited-state quenching that accompanies the electron injection into the conduction band of TiO_2. However, taking into account the fact that the band gap energy of ETS-10 is approximately 0.6 eV higher than that of anatase TiO_2 in water at pH 7.4, the driving force for the electron injection (ca. 0.8 eV) might be reduced to near zero; b) D. Duonghong, J. Ramsden, M. Grätzel, *J. Am. Chem. Soc.* **1982**, *104*, 2977 – 2985.

[13] L. Zang, R. Liu, M. W. Holman, K. T. Nguyen, D. M. Adams, *J. Am. Chem. Soc.* **2002**, *124*, 10640 – 10641.

[14] D. R. James, Y. S. Liu, P. De Mayo, W. R. Ware, *Chem. Phys. Lett.* **1985**, *120*, 460 – 465.

[15] T. Tachikawa, M. Fujitsuka, T. Majima, *J. Phys. Chem. C* **2007**, *111*, 5259 – 5275.

[16] a) M. B. J. Roeffaers, B. F. Sels, H. Uji-i, F. C. De Schryver, P. A. Jacobs, D. E. De Vos, J. Hofkens, *Nature* **2006**, *439*, 572 – 575; b) W. Xu, J. S. Kong, Y.-T. E. Yeh, P. Chen, *Nat. Mater.* **2008**, *7*, 992 – 996.

 © 2009 Wiley-VCH Verlag GmbH & Co. KGaA, Weinheim

These are not the final page numbers!

Communications

Photocatalysis

T. Tachikawa,* S. Yamashita,
T. Majima* _____ ■■■■–■■■■

Probing Photocatalytic Active Sites on a Single Titanosilicate Zeolite with a Redox-Responsive Fluorescent Dye

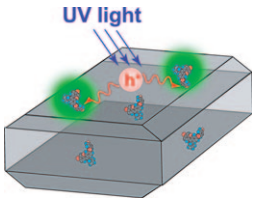

Proper lighting: Investigation of photocatalytic oxidation by in situ fluorescence imaging with a redox-responsive fluorescent dye (see picture, green) shows that acid treatment of single titanosilicate crystals significantly increases both the adsorption and reaction efficiencies and the heterogeneity of photocatalytic activity among crystals. Furthermore, crystal defects serve as reactive sites during the photocatalytic reaction.

© 2009 Wiley-VCH Verlag GmbH & Co. KGaA, Weinheim

Angewandte Chemie
Eine Zeitschrift der Gesellschaft Deutscher Chemiker

Supporting Information

© Wiley-VCH 2009

69451 Weinheim, Germany

Probing Photocatalytic Active Sites on a Single Titanosilicate Zeolite with a Redox-Responsive Fluorescent Dye**

Takashi Tachikawa, Soichiro Yamashita, and Tetsuro Majima**

anie_200904876_sm_miscellaneous_information.pdf

Contents

S1. Experimental Details

Synthesis of ETS-10. ETS-10 was hydrothermally synthesized according to the procedure reported by Yoon et al.[S1] In a typical procedure, concentrated sulfuric acid (2.4 ml, Nacalai Tesque) was added to titanium tetraisopropoxide (5.9 ml, Aldrich) maintained at 0 °C; then, Milli-Q water (35 ml) was slowly added. The mixture was boiled for 3 min at 130 °C and immediately cooled to ~0 °C. This procedure yielded anatase nanoparticles with a diameter of 2-5 nm. The resulting nanoparticle suspension was added to a mixture of sodium silicate (8.5 g, Na_2SiO_3, 36-38% SiO_2, 17-18% Na_2O, Showa Chemical Industry), sodium hydrate (2.6 g, Nacalai Tesque), and Milli-Q water (75 ml) with vigorous stirring. A mixture of potassium fluoride (1.7 g, Wako Pure Chemical Industries) and Milli-Q water (15 ml) was added to this mixture, and the resulting suspension was maintained for 18 h at room temperature. A portion of the suspension (30 ml) was heated in a Teflon-lined stainless steel autoclave at 200 °C for 72 h. The resulting material was separated by centrifugation for 10 min at 10000 rpm, repeatedly washed with Milli-Q water until pH = 7, and then dried overnight at 90 °C.

Powder X-ray diffraction (XRD) and scanning electron microscopy (SEM) measurements have been made using a Rigaku RINT2500 XRD spectrometer with a Kα Cu source and a Hitachi S-2150 instrument operated at an acceleration voltage of 25 kV, respectively.

Hydrofluoric Acid (HF) Treatment of ETS-10. Synthesized ETS-10 powder (0.49 g) was rapidly mixed with 8-wt% hydrofluoric acid (HF) (1.6 ml), and the mixture was vigorously stirred for 3 s and added into excess Milli-Q water (50 ml).[S2] ***Caution!*** *Hydrofluoric acid (HF) is extremely corrosive and a contact poison, and it should be handled with extreme care.* The resulting material was separated by centrifugation for 10 min at 10000 rpm, repeatedly washed with Milli-Q water until pH = 7, and then dried overnight at 90 ºC. The ETS-10 powder treated by HF is denoted as ETS-10(HF).

Sample Preparation. For the single-molecule, single-particle fluorescence measurements, the cover glasses (22 × 22 mm^2) were purchased from Matsunami Glass and cleaned by sonication in a 20% detergent solution (As One, Cleanace) for 6 h, followed by repeated washing with running water for 30 min. Finally, the cover glasses were washed with Milli-Q water. An aqueous suspension of the ETS-10 crystals (3 mg ml^{-1}, pH 7.4, 0.1 M phosphate buffer, 40 μl) was cast on the clean cover glass by spin coating at 2000 rpm for 50 s, followed by annealing the ETS-10 crystals-coated cover glass at 100 °C for 1 h in order for the crystals on the glass not to peel off during the immersion in the solution. After the annealing, the cover glass was repeatedly washed with Milli-Q water and dried with an inert gas. The cover glass was placed on a flow cell built in-house; in this flow cell, the solution in the chamber can be exchanged with other solutions during single-crystal measurements (Figure S1).[S3]

Ensemble Measurements. To evaluate the photocatalytic activity of ETS-10 in bulk solution, 2 ml of 500-nM APF phosphate buffer solution (pH 7.4) containing dispersed ETS-10 crystals (0.5 mg ml^{-1}) was irradiated in a 1 cm × 1 cm quartz cell under continuous stirring; for irradiation, a Hg lamp equipped with

a bandpass (BP) filter (Asahi Spectra, Red Rejection UV Filter RRX340, 290–395 nm, 9 mW cm^{-1}) was used. The fluorescence spectra were measured using a Hitachi 850 spectrofluorometer. All measurements were carried out at room temperature.

Single-Molecule, Single-Crystal Fluorescence Spectroscopy. The experimental setup is based on an Olympus IX71 inverted fluorescence microscope (Figure S1).[S3] The position of the ETS-10 crystal was determined by the transmission image obtained using illumination provided by a 100-W halogen lamp (Olympus, U-LH100L-3) placed above the sample. Light emitted from a continuous wave (CW) Ar ion laser (Melles Griot, 488 nm, 50 mW) was reflected by the first dichroic mirror (Olympus, RDM450) toward the second dichroic mirror (Olympus, DM505); the first mirror reflects wavelengths greater than 450 nm and is transparent to light with wavelengths lesser than 450 nm. CW laser light passing through an objective lens (Olympus, UPlanSApo, 1.40 NA, 100×) after reflection at the second dichroic mirror was used to excite fluorescent probes. For UV-excitation of the sample, light emitted from a 100-W mercury lamp that passed through a BP filter (Asahi Spectra, Red Rejection UV Filter RRX340, 290–395 nm) and a 6% ND filter (Olympus) was made incident on an object lens. The intensity of UV light was ~1 Wcm^{-2} on the cover glass. For imaging, fluorescence was collected using an objective, passed through emission filters to remove undesirable scattered light (Olympus, BA510-550), and imaged by an EM-CCD camera (Roper Scientific, Cascade II:512) at a frame rate of 20 frames s^{-1}. Images were processed using Image-Pro Plus software (Roper Scientific) and ImageJ software (http://rsb.info.nih.gov/ij/). All the experimental data were obtained at room temperature.

Single-Crystal Raman Spectroscopy. The experimental setup is based on an Olympus IX71 inverted fluorescence microscope (Figure S1).[S3] The position of the ETS-10 crystal was determined by the transmission image obtained using illumination provided by a 100-W halogen lamp (Olympus, U-LH100L-3) placed above the sample. A 532 nm CW laser light (Photop Suwtech, DPGL-2050F, 50 mW) passing through an objective lens (Olympus, UPlanSApo, 1.40 NA, 100×) after reflection at a dichroic mirror (Semrock, Di01-R532) was used to excite crystals. The scattered light as well as a background emission was collected using the same objective, passed through an emission filter (Semrock, BLP01-532R-25) to remove scattered excitation light and a slit, and entered the imaging spectrograph (ActonResearch, SP-2356) that was equipped with an EM-CCD camera (Princeton Instruments, PhotonMAX:512B). The spectra were typically integrated for 30 s. The spectrum detected by the EM-CCD camera was stored and analyzed by using a personal computer. The spectral resolution of our detection system was about 12 cm^{-1}. All the experimental data were obtained at room temperature.

***In Situ* Spectroelectrochemical Measurements.** *In situ* spectroelectrochemical measurements were carried out at room temperature using an electrochemical analyzer (ALS, model 660A) with a standard three-electrode configuration. The cell configuration was analogous to that reported by Barbara and co-workers.[S4] A cleaned ITO-coated cover glass (100 nm thickness, 10 Ω cm^{-2}, Matsunami Glass) was used

as a working electrode (WE). The counter electrode (CE) was made by thermal evaporating consecutive thin layers of chromium (15 nm) and gold (70 nm) over a cleaned cover glass using a homemade mask. Two homemade silicone spacers were used to hold the silver wire quasi-reference electrode (QRE) and to create a chamber between the WE and the CE, which was filled with substrate solutions (pH 7.4, 0.1 M phosphate buffer). Electrical connections to the three electrodes were made using silver paint and copper wires. The silver wire QRE potentials were calibrated using ferrocene methanol (FcMeOH, Sigma-Aldrich) as an internal standard that was introduced into the cell after the electrochemical data were acquired. The reported potentials herein are relative to QRE.

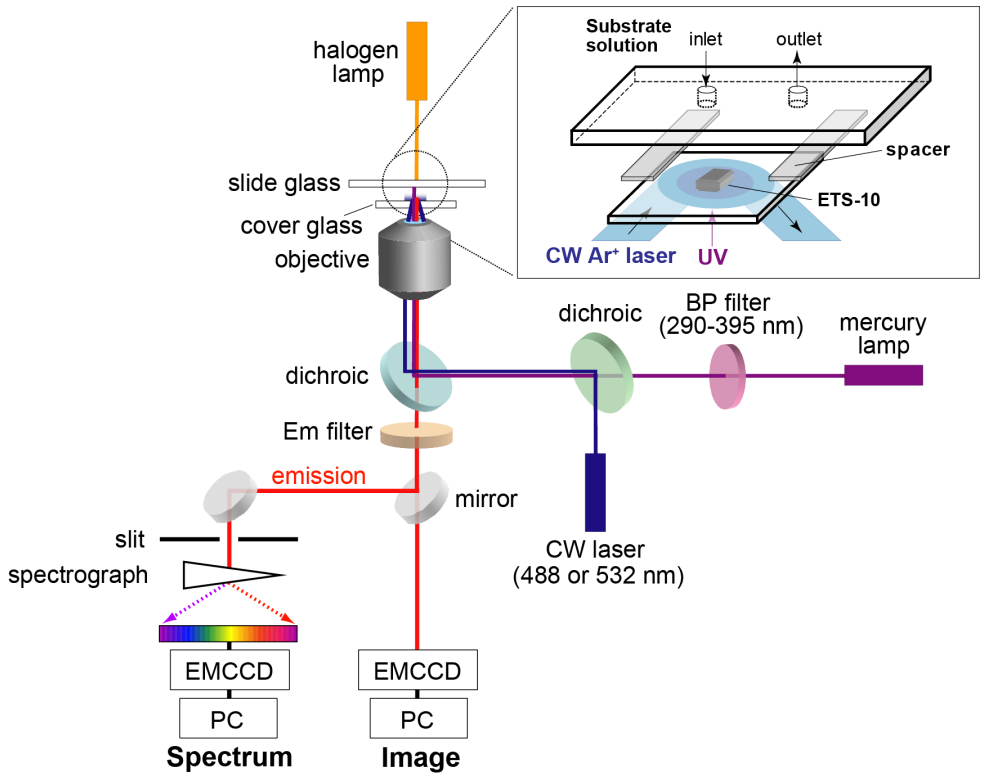

Figure S1. Experimental setup for imaging of photocatalytic reaction occurring on a single ETS-10 crystal using the flow chamber, which is composed of a drilled slide glass and the crystal-immobilized cover glass with a double-sided adhesive spacer. The sample was illuminated by total internal reflection (TIRF) or epifluorescence mode.

S2. Characterizations of ETS-10 Materials

Figure S2A shows the SEM image of as-synthesized ETS-10 powder. The morphology indicated the formation of typical truncated bipyramid crystals similar to those seen in earlier works.[S1,5] The powder XRD pattern of the sample also proved it to be almost pure ETS-10 with a trace impurity of ETS-4 (see asterisks, Figure S2C).[S6,7] As a consequence of HF treatment (8 wt%) for 3 s, the SEM image showed that partial corrosion of external surface occurred for some crystals (Figure S2B), although both the size and morphology of the crystallites remain basically unchanged. Furthermore, the powder XRD pattern of ETS-10(HF) confirmed the formation of anatase TiO_2 in addition to characteristic peaks ascribable to its framework structure (Figure S2D, see arrows). The XRD peaks due to anatase TiO_2 significantly

increased with increasing exposure time of ETS-10 powder to the HF solution. These results are consistent with the finding that the decomposition of the titania wires yields titanium-containing amorphous or anatase nanoparticles.[S8]

Figures S2E and F show the UV-vis diffuse reflectance spectra of ETS-10 powders before and after HF treatment, respectively. The estimated bandgap energies are almost the same for both samples (3.7-3.8 eV), while the tail of absorption edge of ETS-10(HF) shifted to longer wavelength. This result also supports the conclusion that a small amount of anatase TiO_2 (E_g = 3.2 eV) formed during HF treatment.

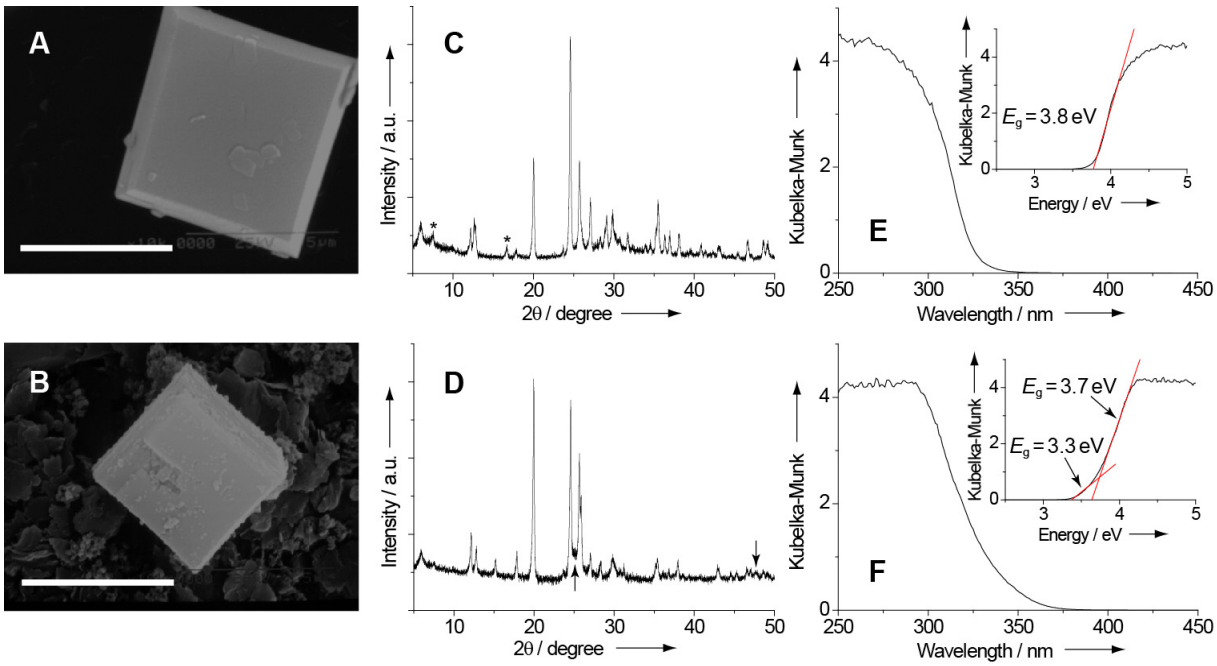

Figure S2. SEM images of ETS-10 crystals before (A) and after HF treatment (B). Scale bars correspond to 5 μm. Powder XRD patterns of ETS-10 crystals before (C) and after HF treatment (D). Peaks assigned to ETS-4 and anatase TiO_2 are indicated by asterisks and arrows, respectively. Steady-state UV-vis diffuse reflectance spectra of ETS-10 crystals before (E) and after HF treatment (F).

S3. Photocatalytic Activity of ETS-10 on an Ensemble

As shown in Figure S3A, the intensity of fluorescence spectra of APF increased gradually upon UV irradiation of phosphate buffer solutions (pH 7.4) containing APF (500 nM) and ETS-10 powder (0.5 mg ml^{-1}). Figure S3B illustrates the time course of fluorescence intensity measured at 514 nm. In the absence of ETS-10, the fluorescence intensity did not increase at all, thus suggesting that the auto-oxidation of APF by the direct UV irradiation can be ruled out under experimental conditions. On the other hand, for sample solutions containing ETS-10 powder, the fluorescence intensity increased with increasing UV irradiation time. These results imply that a fluorescent form of APF molecules is possibly generated from the reaction of photoexcited ETS-10 and APF molecule (see blue circles).

As is well-known, the activity in the photocatalytic degradation of large aromatic molecules of ETS-10 can be enhanced by controlled defect production on the surface with HF treatment. Following the

procedure described by Zecchina et al.,[S2] we treated ETS-10 powders with diluted HF solution (8 wt%) for 3 s, and then measured the fluorescence spectra of buffer solutions containing APF and ETS-10(HF) powder before and after UV irradiation. As expected, a significant increase in fluorescence intensity was observed for ETS-10(HF).

In order to clarify the origin of the generation of the fluorescent form of APF molecule like fluorescein, several experiments were performed as follows: (1) in the presence of DMSO (5 mM) as a $^{\bullet}$OH scavenger, and (2) in the presence of aniline (5 mM) as a co-adsorbate. The former experiment confirmed that approximately 70% fluorescent form was generated by a bimolecular reaction with $^{\bullet}$OH generated during the photocatalytic reaction:

$$^{\bullet}\mathrm{OH} + \mathrm{APF}_{\mathrm{free/ads}} \rightarrow \mathrm{Fl}_{\mathrm{free/ads}}, \qquad \text{(S1)}$$

where "free" and "ads" expressed in the subscript denote free and adsorbed molecules, respectively, and Fl denotes fluorescein molecule. In the later experiment, the generation of the fluorescent form was completely suppressed by the addition of excess aniline, thereby suggesting that APF molecules adsorbed on the surface were directly oxidized by the photogenerated holes in ETS-10.

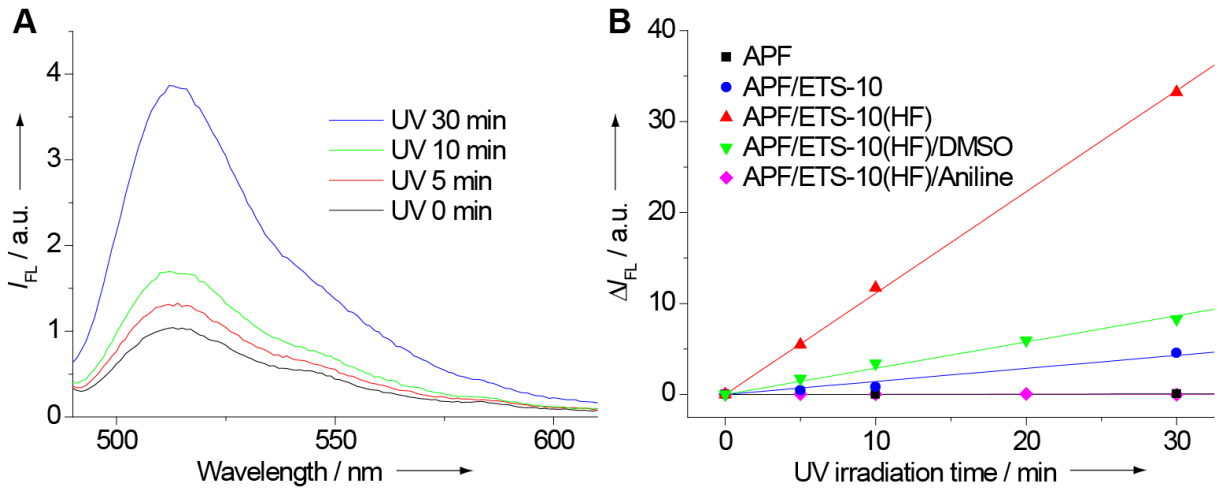

Figure S3. (A) Fluorescence spectra of 500 nM APF phosphate buffer solution (pH 7.4) with dispersed ETS-10 crystals (0.5 mg ml^{-1}) after the UV irradiation. ETS-10(HF) is ETS-10 powder treated with 8-wt% HF solution for 3 s. The excitation wavelength was 460 nm. (B) UV irradiation time dependence of the fluorescence intensity change, which was calculated from fluorescence intensities between before and after UV irradiation, monitored at 514 nm.

S4. Electrochemical Oxidation of Fluorescein

Figure S4 shows the applied potential dependence of the fluorescence intensity (I_{FL}) obtained for the phosphate buffer solution containing fluorescein (500 nM, Nacalai Tesque). The onset of the decrease in the fluorescence intensity at around +0.82 V_{QRE} (= +1.09 V_{NHE}) can be easily correlated to the oxidation potential (E_{ox}) of fluorescein (= +1.1 V_{NHE}).[S9] The silver wire QRE potentials were observed to be ~0.27 V more negative than a Fc^{+}MeOH/FcMeOH couple (= +0.43 V_{NHE}).[S10]

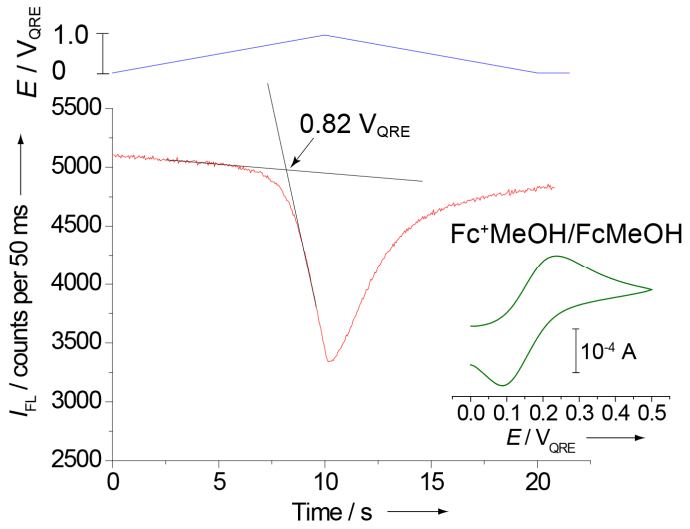

Figure S4. (A) Applied potential dependence of the fluorescence intensity (I_{FL}) obtained for substrate solutions (pH 7.4, 0.1 M phosphate buffer) containing fluorescein (500 nM). Inset shows a typical cyclic voltammogram of ferrocene methanol (FcMeOH) (0.5 mM) in 0.1 M phosphate buffer (pH 7.4) obtained at 0.1 V/s.

S5. APF Concentration Dependence of Fluorescence Intensity

The APF concentration dependence was studied for an identical ETS-10(HF) crystal. As shown in Figure S5, the result showed a clear linear relationship between APF concentration and fluorescence intensity; furthermore, it was estimated that the contribution of scattered light from UV irradiation was ~100 counts. This result suggests that most of emission is attributed to (fluorescent) oxidized APF molecules generated during the UV irradiation.

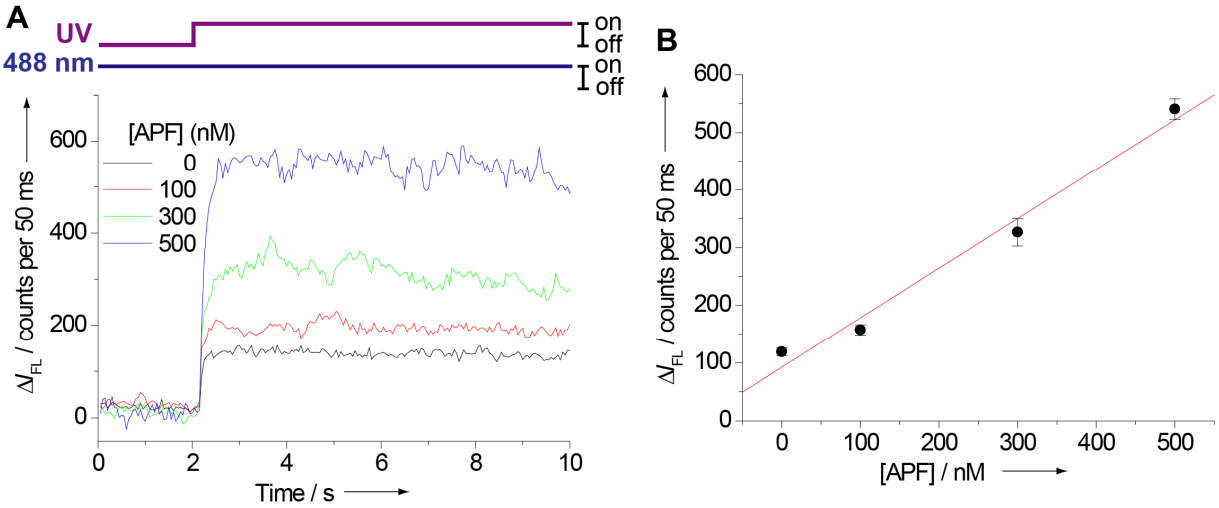

Figure S5. (A) APF concentration ([APF]) dependence of time traces of the fluorescence intensity acquired for ETS-10(HF) in buffer solutions. (B) The relationship between [APF] and fluorescence intensity.

S6. Additive Effects of Aniline and Benzoic Acid

In the presence of aniline (5 mM) as a co-adsorbate, the increase in fluorescence intensity upon UV irradiation was completely suppressed (Figure S6). This result confirmed that the fluorescent form of APF molecules was produced by the one-electron oxidation of adsorbed APF molecules by the

photogenerated holes in ETS-10. We also examined the influence of benzoic acid as a co-adsorbate on the fluorescence intensity upon UV irradiation. We also found that there was no significant difference in fluorescence intensity before and after the addition of benzoic acid (5 mM), thus implying that the *p*-aminophenyl group of APF plays an important role in the adsorption on the surface of ETS-10.

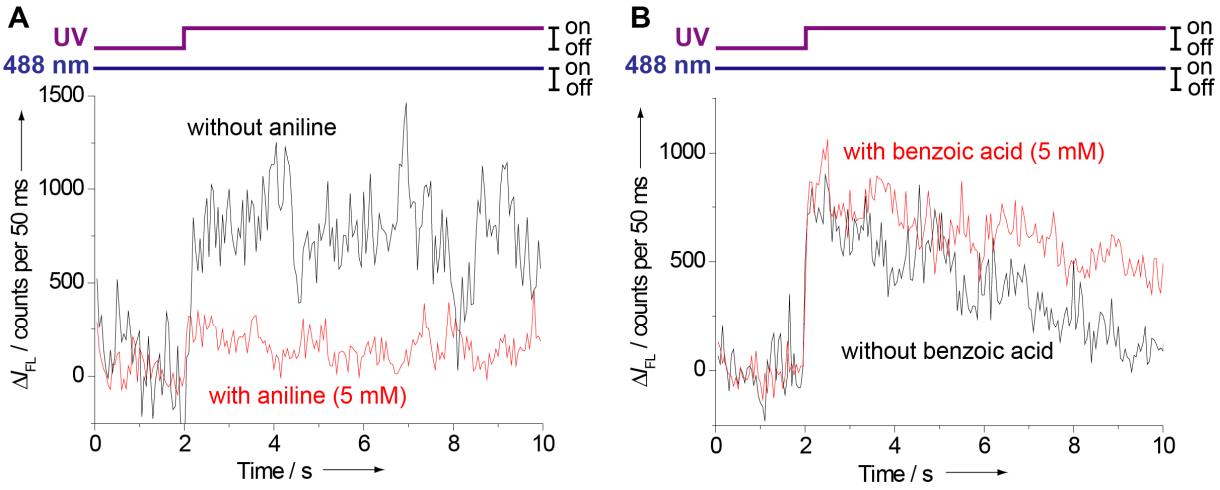

Figure S6. Influences of the addition of aniline (5 mM) (A) or benzoic acid (5 mM) (B) on time traces of the fluorescence intensity acquired for ETS-10(HF) in APF buffer solution (500 nM).

S7. Effect of HF Treatment on an Identical ETS-10 Crystal

Figure S7 shows time traces of the fluorescence intensity acquired for an identical ETS-10 in APF buffer solution (500 nM) before and after HF treatment (1 wt%). After HF treatment, ETS-10 crystals were washed with the same buffer until the eluate was pH 7.4. The increase in fluorescence intensity by HF treatment was directly confirmed for an identical ETS-10 crystal.

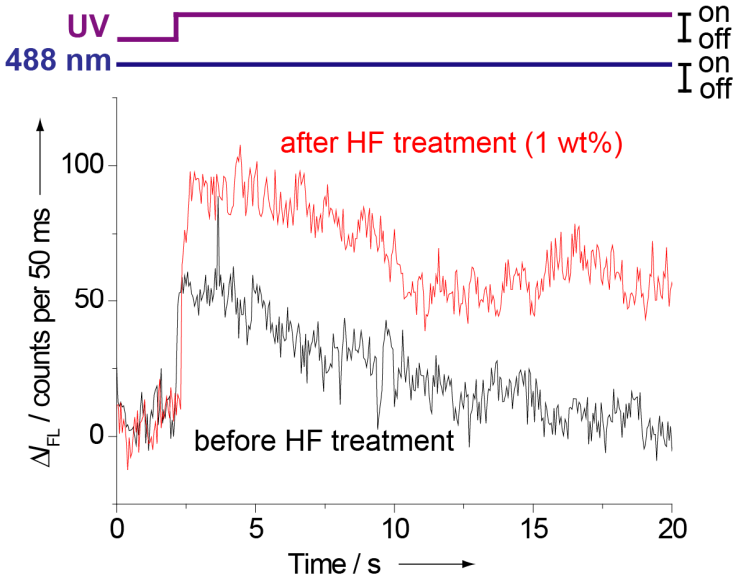

Figure S7. Time traces of the fluorescence intensity acquired for an identical ETS-10 in APF buffer solution (500 nM) before and after HF treatment (1 wt%). In this experiment, the ETS-10 crystal was immobilized on the cover glass surface using agarose gel (1 wt%).

S8. Single-Crystal Raman Spectral Measurements

Bulk Raman or IR experiments only provide ensemble-averaged information on the oxidation (decomposition) process of ETS-10 crystals, suggesting that undesirable contributions of impurities, such as aggregated and cracked crystals, cannot be removed. To distinguish spectroscopically between the decomposed and undecomposed titania wire (-Ti-O-Ti-), therefore, it is noteworthy to observe Raman spectra for individual ETS-10 crystals.

Figure S8A shows Raman spectra observed for single untreated and HF-treated ETS-10 crystals and aggregated anatase TiO_2 nanoparticles (ST-01, Ishihara Sangyo) coated on the cover glass. The Raman spectrum of ETS-10 (black line) shows two bands at <400 and 730 cm^{-1}, which are assigned to a various M-O bending modes (M = Ti or Si) and a collective stretching mode involving the -O-Ti-O-Ti- wires, respectively.[S11] After HF treatment, the band at 730 cm^{-1} is greatly weaken and shifted by up to about 20 cm^{-1} (red line), suggesting the formation of defects on the surface, i.e., interruptions in Ti-O-Ti wires and shortening of the average wire length (Figure S8B).[S11b,c] It should be noted that no peaks assigned to anatase TiO_2 were found for untreated and HF-treated ETS-10 crystals without visible cracks and aggregates (blue line).[S12]

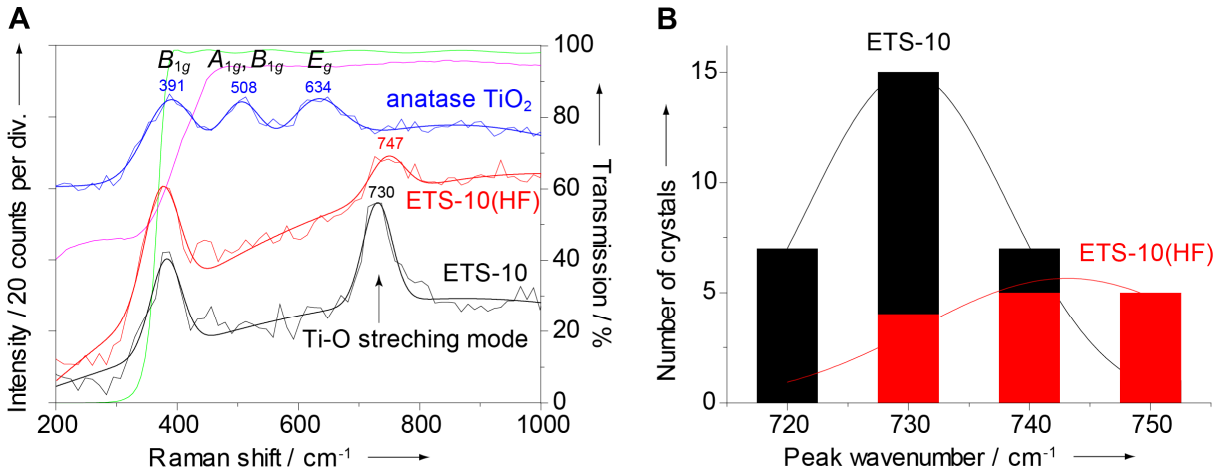

Figure S8. (A) Raman spectra observed for single untreated and HF-treated ETS-10 crystals and aggregated TiO_2 nanoparticles spin-coated on the cover glass. The observed spectra are well fitted by multi-Gaussian functions (bold lines). (Pink and green lines indicate the transmission spectra of the dichroic mirror (Semrock, Di01-R532) and the emission filter (Semrock, BLP01-532R-25) used in this experiment, respectively. (B) Histograms of the peak wavenumber.

S9. Effect of Crystal Defects on the Photocatalytic Oxidation Reactions

Figure S9 shows transmission images (left) and differential fluorescence images (right), which are calculated by subtracting the image acquired before UV irradiation from the image acquired after UV irradiation, observed for ETS-10 (A) and ETS-10(HF) (B) crystals. The increase in fluorescence intensity observed at the defect upon UV irradiation is considerably higher than the increase observed at other areas.

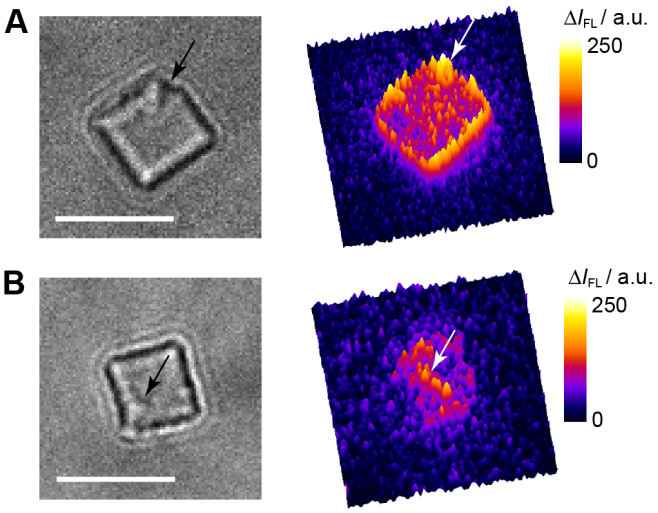

Figure S9. Transmission images (left) and differential fluorescence images (right), which are calculated by subtracting the image acquired before UV irradiation from the image acquired after UV irradiation, observed for ETS-10 (A) and ETS-10(HF) (B) crystals. Scale bars correspond to 5 μm. Arrows indicate the location of crystal defects.

References

[S1] N. C. Jeong, M. H. Lee, K. B. Yoon, *Angew. Chem.* **2007**, *119*, 5972-5976; *Angew. Chem. Int. Ed.* **2007**, *46*, 5868-5872.

[S2] F. X. Llabrés i Xamena, P. Calza, C. Lamberti, C. Prestipino, A. Damin, S. Bordiga, E. Pelizzetti, A. Zecchina, *J. Am. Chem. Soc.* **2003**, *125*, 2264-2271.

[S3] K. Naito, T. Tachikawa, M. Fujitsuka, T. Majima, *J. Am. Chem. Soc.* **2009**, *131*, 934-936.

[S4] R. E. Palacios, F.-R. F.Fan, A. J. Bard, P. F. Barbara, *J. Am. Chem. Soc.* **2006**, *128*, 9028-9029.

[S5] M. W. Anderson, O. Terasaki, T. Ohsuna, P. J. O. Malley, A. Philippou, S. P. MacKay, A. Ferreira, J. Rocha, S. Lidin, *Philos. Mag. B* **1995**, *71*, 813-841.

[S6] M. W. Anderson, O. Terasaki, T. Ohsuna, A. Philippou, S. P. MacKay, A. Ferreira, J. Rocha, S. Lidin, *Nature* **1994**, *367*, 347-351.

[S7] S. M. Kuznicki, V. A. Bell, S. Nair, H. W. Hillhouse, R. M. Jacubinas, C. M. Braunbarth, B. H. Toby, M. Tsapatsis, *Nature* **2001**, *412*, 720-724.

[S8] Y. K. Krisnandi, E. E. Lachowski, R. F. Howe, *Chem. Mater.* **2006**, *18*, 928-933.

[S9] J. Suomi, T. Ylinen, M. Hakansson, M. Helin, Q. Jiang, T. Ala-Kleme, S. Kulmala, *J. Electroanal. Chem.* **2006**, *586*, 49-55.

[S10] a) E. Madej, P. Wardman, *Radiat. Phys. Chem.* **2006**, *75*, 990-1000; b) P. Vuorilehto, *J. Appl. Electrochem.* **2008**, *38*, 1427-1433.

[S11] a) Y. Su, M. L. Balmer, B. C. Bunker, *J. Phys. Chem. B* **2000**, *104*, 8160-8169; b) P. D. Southon, R. F. Howe, *Chem. Mater.* **2002**, *14*, 4209-4218; c) C. C. Pavel, S.-H. Park, A. Dreier, B. Tesche, W. Schmidt, *Chem. Mater.* **2006**, *18*, 3813-3820.

[S12] a) U. Balachandran, N. G. Eror, *J. Solid State Chem.* **1982**, *42*, 276-282; b) J. Mizuguchi, T. Shinbara, *J. Appl. Phys.* **2004**, *96*, 3514-3519.